Title
PREDICTION OF EROSIVE WEAR BY SOLID PARTICLES IN A TURBULENT CURVED CHANNEL FLOW

Authors
Humphrey, J.A.C.
Pourahmadi, F.
Levy, A.

Publication Date
1983-05-01

Lawrence Berkeley Laboratory
UNIVERSITY OF CALIFORNIA

Materials & Molecular
Research Division

Presented at the 7th Annual Conference on Materials for Coal Conversion and Utilization, Gaithersburg, MD, November 16-18, 1982

PREDICTION OF EROSIVE WEAR BY SOLID PARTICLES IN A TURBULENT CURVED CHANNEL FLOW

J.A.C. Humphrey, F. Pourahmadi, and A. Levy

May 1983

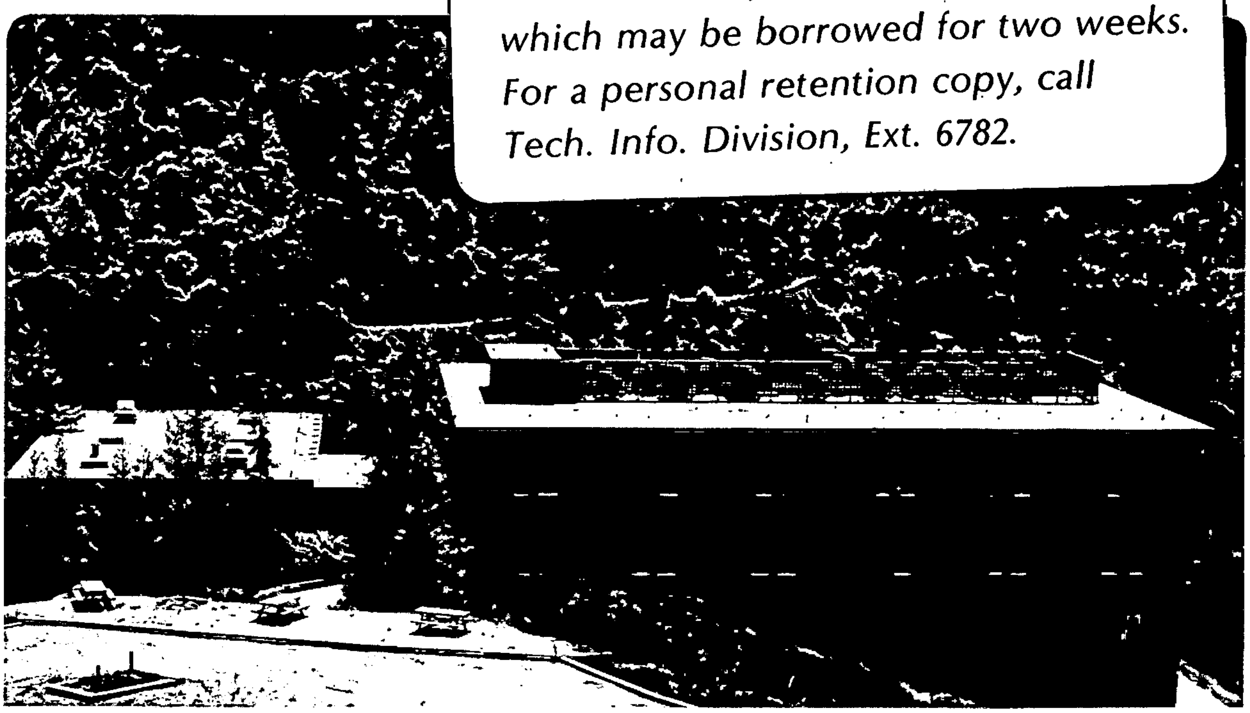

Prepared for the U.S. Department of Energy under Contract DE-AC03-76SF00098

PREDICTION OF EROSIVE WEAR BY SOLID PARTICLES IN A TURBULENT CURVED CHANNEL FLOW

J. A. C. Humphrey[1] and F. Pourahmadi[2]

Department of Mechanical Engineering
University of California, Berkeley
Berkeley, California 94720

and

A. Levy[3]

Materials and Molecular Research Division
Lawrence Berkeley Laboratory
University of California, Berkeley
Berkeley, California 94720

Presented at the
Seventh Annual Conference
on
Materials for Coal Conversion and Utilization

November 16-18, 1982

National Bureau of Standards
Gaithersburg, Maryland

1 Assistant Professor
2 Research Graduate Student
3 Senior Scientist

CONTENTS

Abstract

1. Introduction
1.1 The Problem(s)
1.2 Earlier Work and Modeling Approaches
1.3 The Influence of Turbulence
1.4 Summary

2. The Numerical Model
2.1 Assumptions
2.2 Modeled Transport Equations
2.3 Boundary Conditions
2.4 The Erosion Model
2.5 The Solution Algorithm

3. Results and Discussion
3.1 Numerical Model Testing
3.2 Application to Curved Channel Flow

4. Conclusions

Acknowledgements

References

Notation

Tables

Figures

PREDICTION OF EROSIVE WEAR BY SOLID PARTICLES IN A TURBULENT CURVED CHANNEL FLOW

J. A. C. Humphrey and F. Pourahmadi

Department of Mechanical Engineering
University of California, Berkeley

and

A. Levy

Materials and Molecular Research Division
Lawrence Berkeley Laboratory
University of California, Berkeley

Numerical modeling of fluid-particulate turbulent flow transport processes, including erosion, cannot substitute (at least for the present) good experimentation. Notwithstanding, the calculation approach offers a viable, relatively inexpensive and complementary alternative for gleaning useful information on the relative dependence of particle transport and erosion on the flow system parameters of relevance. In the present study these parameters include: the particle phase response time, Reynolds number and concentration; the turbulent characteristics of the fluid phase; the channel aspect ratio and curvature. This communication summarizes the main results predicted by means of a numerical procedure for the motion of a dilute suspension of solid particles driven by turbulent flow in curved and straight two-dimensional channels. An exposition of the theoretical development, the numerical model, its testing and application to these configurations of special engineering interest are provided. A simple model for erosion is used successfully to predict surface wear.

1. Introduction

1.1 The Problem(s)

The problem of erosive wear by solid particulates suspended in a turbulent flow is of fairly obvious practical importance. Two-phase flows cover a wide spectrum of applications in many areas, ranging from numerous engineering applications to a variety of processes associated with natural flows. The dispersion of dust and pollutant particulates in the atmosphere, the transport of silt and fine mineral particles by rivers, the erosion of pipeline components in coal liquefaction/gasification systems, and also the erosion of gas turbine blades and internal walls of nozzles in solid-propellant rockets are but a few examples of the diversified processes which are affected by the motion of two-phase turbulent flows. Other engineering examples of strong relevance to this work are: fluidized beds, pneumatic conveying, settling tanks, sand blasting, the flow of slurries and fibers and the flows occuring in cyclone separators and electrostatic precipitators. The flows of particle-laden fluids in coal liquefactoin/gasification pipeline systems cause erosion of the wall materials. This can result in serious damage and possible catastrophic failures, both from the safety and economical points of view. For coal liquefaction/gasification systems the problem of erosive wear is quite severe at pipe bends, tee junctions and impinging jet surfaces. The successful design and determination of optimum operation conditions of such systems requires measurement, analysis and prediction of the fluid mechanical characteristics of the turbulent two-phase flows in the components comprising the systems. Due to the complexity of the fundamental aspects governing particle motion and wear by impingement, these topics are also of considerable academic interest.

Experimental studies of particle-laden turbulent flows are indispensable for identifying and quantifying the mechanisms controlling particle transport and particle-surface interactions. Unfortunately, experiments are often costly, laborious and time-consuming to perform. Often they cannot be executed to the degree of spatial and temporal resolution required to help unravel the sequence and nature of the physical mechanisms involved.

The large storage capacities and rapidity of calculation typical of digital computers today make attractive the numerical modeling approach for studying particle-laden turbulent flows. The availability of a computational model allows "numerical experiments" to be performed with relative ease, often at a fraction of the cost (and certainly at a microfraction of the time!) entailed by the corresponding laboratory experiment. While the lure is strong to pursue this approach, unfortunately it is fraught with its own impedimenta. The difficulties are mainly two. The first and less serious is related to numerical accuracy. A computational model must be based on a stable and accurate numerical scheme, in order to allow a proper assessment of the model physics. In principle, most complications (if not all) which are strictly numerical can be solved, therefore they will not concern us here. The second difficulty arises in connection with the model(s) chosen to represent the various physical aspects of the problem. Present-day theoretical knowledge of turbulent two-phase flow behavior is inadequate so that, by necessity, models of the physical characteristics of such flows must reflect the inadequacies. In spite of this second, much more serious limitation, the financial incentives are very strong for using the computational approach to predict particle motion and erosive wear. Therefore, it becomes imperative to conduct careful, selective experimentation in parallel with the necessary theoretical developments. If properly planned, selective experimentation can yield: i) data to help understand and formulate fundamental mechanisms; and, ii) data of value for testing mathematical models representing these mechanisms. Because of the different nature of these two requirements, the two sets of data are not necessarily the same.

Given the undesirably large gaps and serious limitations in present day knowledge of two-phase flow behavior, we are led to conclude that an especially strong synergic interaction is required between research programs respectively aimed at the experimental measurement and the mathematical (numerical) modeling of these flows. The present contribution focuses on the achievements and limitations of a particular numerical model, within the context of a broader program of research which includes experimentation. After a brief discussion addressing earlier work and the influence of turbulence, the model is outlined briefly and the principal results obtained for the turbulent, erosive flow of particulates in a curved channel are presented and discussed. The paper closes with some general conclusions and recommendations for future work.

1.2 Earlier Work and Modeling Approaches

In the course of reviewing the literature on two-phase fluid-particulate flows, the variety of investigations and the range of complexity of the analyses is found to be amazingly large. Many significant contributions have been cited in the books by Soo [1] and Boothroyd [2], and in the sequence of reviews given by Torobin and Gauvin [3-5]. The motion of a dispersed particulate phase in a continuous fluid phase has been analyzed by both Lagrangian and Eulerian methods. In the Lagrangian approach, the dynamics of single particles are analyzed by following the motion of these with a prescribed set of initial conditions. In the Eulerian approach the two-phase flow can be considered as two interacting continua, with separate boundary conditions for each phase. The success of either approach for the prediction of the flow variables of interest depends on the appropriate inclusion and accurate modeling of the various and relatively complex physical processes represented in the governing equations. The occurrence of fluid turbulence, and the associated solid phase turbulence implying complex interactions and exchange mechanisms between the two phases, can be fairly significant and requires proper modeling.

Continuum-type approaches can be roughly divided into two categories. In the first, the two-phases are treated as separate, interacting continua, in which, for the particulate phase, a diffusional mode of transport, as well as convection, are included. In this respect, the following investigations are noteworthy: Soo [6], Drew [7], Hinze [8] for laminar flow, and Hinze [9], Drew [10], Nagarajan [11] and Soo [12] for turbulent flow. In the second approach, the two-phase flow is treated as a single continuum in which fluid variables are redefined to include the presence of the particulate phase. Formulations following this approach have been given by Wallis [13] and Hinze [8] and are common in gas/liquid flows with mass exchange between the phases. Wallis [13] has shown that for such an approach to be valid the assumption of dynamical and thermal equilibrium between the phases must be made which is approximately valid only for very small particles and low flow velocities.

In the Lagrangian approach, the motion of single particles are considered and relevant variables are calculated along the particle trajectories. Early works based on Lagrangian equations of motion are due to Glauert [14], Langmuir and Blodgett [15], and Brun and Mergler [16] in relation to the impingement of rain-drops on aircraft surfaces for the analysis of ice formation on aircraft wings. Other more recent investigations using this approach are those due to Laitone [17], Yeung [18] and Abuaf and Gutfinger [19].

In the present work, because it is more convenient to analyse the flow through engineering systems in terms of fixed coordinates, attention will be restricted to a formulation following the Eulerian approach.

1.3 The Influence of Turbulence

In the presence of turbulence, the problem of measuring and/or predicting two-phase flows becomes even more complicated. A successful prediction requires a thorough understanding and proper modeling of all major turbulence-related processes. It is clear that, for this, a detailed understanding of the fundamentals of fluid and particulate phase turbulence, including significant fluid-particle interactions, is required. In this regard the investigation of Baw and Peskin [20] can be mentioned. In their study particle effects on the fluid turbulence energy spectrum were analyzed and the results showed increased reductions in the spectrum values with increases in wave-number, compared to the pure fluid spectrum. In a related work, Owen [21] has shown a reduction in fluid turbulence intensity with increases in particle concentration. However, this result was not observed by Soo et al. [22] who noticed no effect due to the presence of particles. An increase in dissipation rate of turbulent kinetic energy with particulate concentration has been reported by Kada and Hanratty [23], Owen [21], and Hino [24]. In the last two investigations, a decrease in eddy diffusivity with particle concentration was observed which contrasts with the results given by Kada and Hanratty [23].

A review of some fundamental problems arising in turbulent two-phase flows has been given by Peskin [25]. Particle effects on fluid mean velocity have been investigated by Soo [26-28], Peskin [29-30] and Peskin and Dwyer [31] in pipe flow. The results show a flattening of the fluid velocity profile induced by the solid particles, even at small concentrations of the particulate phase. Soo et al. [22] have shown a decrease in the Lagrangian integral scale with an increase in particulate concentration. Other studies aimed at measuring the mean flow characteristics of confined two-phase turbulent flows are given in [32-39].

In spite of the lack of detailed fundamental knowledge required for the formulation and modeling of two-phase turbulent flows, the need to predict flows of industrial interest has stimulated analyses for obtaining approximate solutions for these flows. Drew [40] has modeled the problem of turbulent sediment transport over the flat bottom of a stirring tank in which the mixing length hypothesis was used. Nagarajan and Murgatroyd [41] have presented an analytical model for two-phase turbulent flow in a fully-developed pipe flow. The assumption of a linear variation of the turbulent shear stress in the radial direction, the neglect of all but the dissipation and production terms in the turbulence kinetic energy equation, and the introduction of several empirical and configuration-dependent coefficients make their solution too specific for general applications. In a related work, the effects due to gravity and electrostatic effects were later included by Nagarajan [11]. Based on the single-continuum model approach, Kramer and Depew [42] developed a calculation model for fully developed two-phase turbulent pipe flows. To obtain a solution, they expressed velocity fields in terms of various empirical coefficients and in addition an assumption of linear mixing length was made. Yuu et al. [43] developed a solution for two-phase turbulent jet flows. In their calculations they substituted empirical relations for the fluid mean velocities in the Lagrangian equations for the motion of the particles.

Smith et al. [44] have presented a two-dimensional Lagrangian model for dilute particulate flows in which the fluid variables are obtained using a two-equation (k-ε) model of turbulence, but without considering particle effects on the fluid turbulence. Danon et al. [45] have presented a turbulence model for two-phase turbulent flows which is based on a set of parabolic conservation equations. In their model the particulate phase mean velocity is not solved directly but is assumed to be equal to the fluid velocity. In order to avoid complex particulate-wall interaction effects, the model was applied to axi-symmetric free jet flows only. The fluid Reynolds stresses were modeled using fluid turbulent length scale and fluid turbulent kinetic energy concepts. For the turbulent length scale, an algebraic relation was assumed which remained constant in the lateral directions, and the fluid turbulent kinetic energy was obtained from a parabolic conservation equation in which particulate interaction effects with the fluid were included. However, the closure relation for the fluid-particle correlation term was assumed to be of an exponential form and was not rigorously derived. Finally, for obtaining better agreement with the data for turbulent kinetic energy, the dissipation and production terms were assumed to have a linear variation with particulate concentration. This assumption, however, resulted in the introduction of two new empirical constants which were dependent on particle size and were "tuned" to match the experimental data.

Genchev and Karpuzov [46] have proposed a turbulence model for fluid-particle flows in which the effect of particles in the turbulence transport equations are considered. The assumptions of uniform particulate concentration and equivalence of particle-phase mean velocity to the fluid velocity simplified the problem by making it possible to discard the governing equations for particulate phase concentration and momentum. These assumptions, of course, have limited the range of applicability of the model. In the Genchev and Kapuzov model, the closure for fluid Reynolds stresses is based on the eddy viscosity concept proposed by Harlow and Nakayama [47] in which transport equations for the fluid turbulent kinetic energy and a turbulent length scale are solved. Despite the inclusion of particle effects in the turbulent fluid transport equations, the fluid-particle correlation terms were assumed to be negligible in comparison with their fluid-fluid counterparts. This simplification obviates the need to account for the complex fluid-particle correlation terms. As argued by the authors, the assumption is valid if typical particle response times are much larger than the time scale characteristic of the mean fluid motion. However, the last assumption regarding time scales is in conflict with the earlier assumption regarding equal fluid and particulate mean velocities. For the equal velocity condition the particle response time must be much smaller than the mean fluid motion time scale. Thus, the assumption which makes it possible to avoid the complexity of the fluid-particle interaction terms raises a serious inconsistency in the model. Finally, the authors applied their turbulence model to the case of fully-developed pipe flow, but no experimental data was provided in order to evaluate the capabilities and limitations of the model.

1.4 Summary

As discussed above, calculation methods for two-phase turbulent flows invariably embody numerous simplifying assumptions in order to allow solutions for the flow field variables. In the majority of the analytical studies listed above, particulate phase effects on the fluid turbulence structure have not been considered. In the few investigations where such effects have been incorporated, further simplifications in the governing turbulence equations became necessary, and various empirical coefficients were introduced. The latter are, in general, functions of the flow characteristics and yield calculation schemes which are strictly valid only for the flow conditions for which they were optimized. Such schemes are not readily extended to encompass more general flow conditions and configurations.

The objective of this work is to analyze two-phase turbulent flow with the view of developing a more general turbulence model for computing flows of engineering interest. The model will be based on the two-equation (k-ε) model of turbulence for single-phase flows with universal constants [48]. The governing transport equations for the particulate and fluid phases are taken in their fully-elliptic forms, in order not to preclude the possibility of predicting flow recirculation. In the momentum balance equations, the interactive effects of the two phases are considered and, in addition, particulate phase momentum exchanges with solid walls are included. The inclusion of the latter effect enhances further the capability of the present model for predicting wall-bounded flows which frequently arise in practice. The various fluid-particulate correlation terms in the equations for fluid turbulent kinetic energy and its dissipation rate are rigorously modeled using the governing equation for the particulate-phase fluctuating velocity.

Ultimately, the numerical model developed in this investigation will be used to predict various two-phase flow quantities as well as erosive wear by solid particulates in curved and straight two-dimensional channel flows. The tested and validated calculation procedure can be viewed as a relatively inexpensive and very valuable tool for conducting two-phase flow and erosive wear "experimentation"; not only in curved channels, but in other shapes such as sharp bends, tees, backward- and forward-facing steps, axisymmetric contractions and expansions, and curved solid objects immersed in a free flow, to name a few. While such a computational tool is more economical than experimentation, it cannot be looked upon as a substitute for experiments. The foundations of the model depend on critical experimentation, and validation of the model requires appropriate test data. Notwithstanding, in many systems of engineering interest, especially newly conceived ones, often the data required to characterize the system is not available, and to conduct detailed experiments can be prohibitively expensive or time consuming. In such cases the tool provided here is of most use. While in absolute terms calculations of an unknown two-phase flow may not be verifiable until experimental data is available, relative comparisons of parametric effects can still be extremely useful for alterning and/or optimizing the system characteristics and enhancing its performance. It is in this spirit that the present study has been motivated.

2. The Numerical Model

This section is devoted to listing the assumptions and the forms of the modeled transport equations with appropriate boundary conditions for predicting dilute, turbulent, two-phase flow and erosion in straight and curved two-dimensional channels. The solution methodology and numerical algorithm are also outlined. The brief description provided here is based on the more complete exposition given by Pourahmadi [49].

2.1 Assumptions

The following assumptions are implied in the modeled form of the equations given below:

1. The particulate phase if taken to be a continuum and treated as such.
2. The fluid phase is taken to be Newtonian.

3. The flow is steady, incompressible and isothermal.
4. Fluid and particulate phase properties are constant.
5. The particle phase response time, τ_m, is calculated by departing from the continuum assumption and analyzing spherical particles of diameter d_p.
6. Momentum exchange between the fluid and the particulate phase is through Stoke's viscous drag only.
7. The particulate phase is dilute, meaning that the volume concentration, α, is $\alpha << 1$.
8. The flow is locally isotropic, and viscous diffusion is negligible compared to turbulent diffusion at high Reynolds number, Re.
9. Brownian and Bernouillian diffusion of the particulate phase are negligible compared to turbulent diffusion induced by the fluid motion.
10. Third-order correlations containing particle concentration fluctuations are negligible.

2.2 Modeled Transport Equations

The equations listed below have been derived by Pourahmadi [49] using Reynolds decomposition for fluctuating variables and time averaging of the instantaneous equations. These equations are in agreement with those given by Hinze [8] if the flow resistance of the particulate phase is modeled according to assumption 6. Although programmed in cylindrical coordinates for curved channel flow predictions, and in cartesian coordinates for straight channel flow, the equations are given here in cartesian notation for compactness of presentation. The summation convention on repeated indices is implied.

Mass Conservation Equations

a) Fluid Phase

$$\frac{\partial U_{f_i}}{\partial x_i} = 0 \qquad (1)$$

b) Particulate Phase

$$\frac{\partial}{\partial x_i} (\alpha \, U_{p_i} + \overline{\alpha' u_{p_i}}) = 0 \tag{2}$$

In Eq. (2) the second term represents a mass flux contribution due to turbulent diffusion of the particulate phase. Following Hinze [9], we assume a gradient-type diffusion for this correlation given by:

$$\overline{\alpha' u_{p_i}} = - \nu_{t_p} \frac{\partial \alpha}{\partial x_i} \tag{3}$$

In Eq. (3) ν_{t_p} represents the turbulent diffusivity for particulate mass concentration and is taken as a fraction of the fluid turbulent viscosity, ν_{t_f}. It is modeled along the lines of Peskin [30]:

$$\frac{\nu_{t_p}}{\nu_{t_f}} = 1 - \frac{T_L^2}{15} \frac{\varepsilon}{\nu} \frac{3K^2}{K+2} \tag{4}$$

where,

$$K = \frac{2\tau_m}{T_L} \tag{5}$$

is the ratio of particle response time to the fluid Lagrangian integral time scale. These quantities are respectively given by:

$$\tau_m = \frac{\tilde{\rho}_p \, d_p^2}{18\mu} \tag{6}$$

and

$$T_L = C_T \, k/\varepsilon \tag{7}$$

with C_T an experimental constant equal to 0.41. For fast particulate phase response times ($\tau_m \to 0$) we have $\nu_{t_p} \simeq \nu_{t_f}$.

Momentum Balance Equations

a) Fluid Phase

$$\tilde{\rho}_f \frac{\partial}{\partial x_j} (U_{f_i} U_{f_j}) = - \frac{\tilde{\rho}_p}{\tau_m} \Big[\underset{(A)}{\alpha (U_{f_i} - U_{p_i})} + \underset{(B)}{\overline{\alpha' (u_{f_i} - u_{p_i})}} \Big] - \frac{\partial}{\partial x_j} (P \, \delta_{ij}) + \tilde{\rho}_f \frac{\partial}{\partial x_j} \left(\nu_{t_f} \frac{\partial U_{f_i}}{\partial x_j} \right) \quad (8)$$

In Eq. (8) the Boussinesq assumption has been used for expressing the Reynolds stresses:

$$- \overline{u_{f_i} u_{f_j}} = \nu_{t_f} \left(\frac{\partial U_{f_i}}{\partial x_j} + \frac{\partial U_{f_j}}{\partial x_i} \right) - \frac{2}{3} \delta_{ij} k \quad (9)$$

where $k = 1/2 \, (\overline{u_{f_i} u_{f_i}})$ is the fluid turbulent kinetic energy and ν_{t_f} is the flow turbulent viscosity. In the two-equation k-ε model of turbulence [48-50], the latter quantity is related to k and the rate of dissipation of k(ε) by:

$$\nu_{t_f} = C_\mu \frac{k^2}{\varepsilon} \quad (10)$$

with $C_\mu = 0.09$.

The fluid-particle interaction in Eq. (8) comprises two terms. The first term (A) represents the mean viscous drag induced by the particulate phase, the second term (B) is the drag contribution induced by the turbulent diffusion of the particulate phase.

It has been postulated by Hinze [9] and Davidson and McComb [51] that:

$$\overline{\alpha' u_{f_i}} = - \nu_{t_\alpha} \frac{\partial \alpha}{\partial x_i} \tag{11}$$

with ν_{t_α} denoting the turbulent diffusivity for the transport of the scalar α. An investigation of the behavior of $\overline{\alpha' u_{f_i}}$ in [49] suggests that, to a good approximation:

$$\overline{\alpha' u_{f_i}} = \overline{\alpha' u_{p_i}} \tag{12}$$

and will so be modeled. In effect, the approximation implies that A >> B in Eq. (8).

b) Particulate Phase

$$\frac{\partial}{\partial x_j} (\alpha \, U_{p_i} U_{p_j}) = \frac{1}{\tau_m} \alpha (U_{f_i} - U_{p_i}) \atop (A_1)$$

$$- \frac{\partial}{\partial x_j} \left[- \alpha \nu_{t_p} \left(\frac{\partial U_{p_i}}{\partial x_j} + \frac{\partial U_{p_j}}{\partial x_i} \right) + \frac{2}{3} \alpha \delta_{ij} \left(k_p + \nu_{t_p} \frac{\partial U_{p_\ell}}{\partial x_\ell} \right) \right]$$

$$- \frac{\partial}{\partial x_j} \left[\nu_{t_p} \left(U_{p_j} \frac{\partial \alpha}{\partial x_i} + U_{p_i} \frac{\partial \alpha}{\partial x_j} \right) \right] \tag{13}$$

In Eq. (13) the approximation given by Eq. (12) has been used and the Boussinesq approximation given by Eq. (9) has been extended to the particulate phase:

$$- \overline{u_{p_i} u_{p_j}} = \nu_{t_p} \left(\frac{\partial U_{p_i}}{\partial x_j} + \frac{\partial U_{p_j}}{\partial x_i} \right) - \frac{2}{3} \delta_{ij} \left(k_p + \nu_{t_p} \frac{\partial U_{p_\ell}}{\partial x_\ell} \right) \tag{14}$$

The divergence term in Eq. (14) is required to ensure $\overline{u_{p_i} u_{p_i}} = 2 \, k_p$.

Note that term A_1 is equal in magnitude but opposite in sign to term A in Eq. (8), thus showing clearly the mean momentum exchange between the two phases.

Turbulent Kinetic Energy

a) Fluid Phase $\left(k \equiv \frac{1}{2}\,\overline{u_{f_i} u_{f_i}}\right)$

$$U_{f_j} \frac{\partial k}{\partial x_j} = \frac{\partial}{\partial x_j}\left(\frac{\nu_{t_f}}{\sigma_k}\frac{\partial k}{\partial x_j}\right) - \overline{u_{f_i} u_{f_j}}\,\frac{\partial U_{f_i}}{\partial x_j} - \varepsilon$$
$$- \frac{\tilde{\rho}_p}{\tau_m}\Big[\underbrace{\alpha\left(\overline{u_{f_i} u_{f_i}} - \overline{u_{f_i} u_{p_i}}\right)}_{(A_2)} + \underbrace{\overline{\alpha' u_{f_i}}\left(U_{f_i} - U_{p_i}\right)}_{(B_2)}\Big] \tag{15}$$

In this equation σ_k is the "Prandtl" number for k and is taken as $\sigma_k = 1.0$ [50]; ε is the isotropic rate of dissipation of k; $\overline{u_{f_i} u_{f_j}}$ and $\overline{\alpha' u_{f_i}}$ are modeled according to Eqs. (9) and (12) respectively; and,

$$\overline{u_{f_i} u_{p_i}} \simeq 2k \frac{T_L}{\tau_m + T_L} \tag{16}$$

The form of Eq. (16) has been derived by Pourahmadi [49] by reference to the Lagrangian equation of motion for a single particle and is limited to high flow Reynolds numbers, short particle response times, and dilute systems.

As argued in [49], term A_2 in Eq. (15) represents a transfer of kinetic energy of turbulence of the fluid phase to kinetic energy of the particulate phase. Term B_2 also represents an energy transfer term, from the mean kinetic energy of the fluid phase to the turbulent kinetic energy of the particulate phase *via* the turbulent kinetic energy of the fluid phase.

b) Particulate Phase $\left(k_p \equiv \frac{1}{2}\overline{u_{p_i}u_{p_i}}\right)$

The equation for turbulent kinetic energy of the particulate phase has been derived in [49]. However, the complexity of the various correlations it contains precludes a direct solution for k_p. For high flow Reynolds numbers, short particle response times and dilute systems:

$$k_p \simeq k \frac{T_L}{\tau_m + T_L} \tag{17}$$

The form of this relation implies that the fluid turbulence is the only source of energy for turbulence in the particulate phase, and that the turbulent kinetic energy exchange between the two phases is through viscous interaction.

Isotropic Dissipation of k for the Fluid Phase $\left(\varepsilon \equiv \nu \overline{\frac{\partial U_{f_i}}{\partial x_j}\frac{\partial U_{f_i}}{\partial x_j}}\right)$

The modeled form of the equation for ε derived in [49] is:

$$U_{f_j}\frac{\partial \varepsilon}{\partial x_j} = \frac{\partial}{\partial x_j}\left(\frac{\nu_{t_f}}{\sigma_\varepsilon}\frac{\partial \varepsilon}{\partial x_j}\right) - C_1 \frac{\varepsilon}{k}\overline{u_{f_i}u_{f_j}}\frac{\partial U_{f_i}}{\partial x_j}$$

$$- C_2 \frac{\varepsilon^2}{k} - \tilde{\rho}_p \frac{\alpha}{\tau_m}\left[\varepsilon - \underbrace{\nu \overline{\frac{\partial u_{f_i}}{\partial x_j}\frac{\partial u_{p_i}}{\partial x_j}}}_{(A_3)}\right] . \tag{18}$$

In the absence of particles $\alpha = 0$ and Eq. (18) reduces to the accepted form for a single phase turbulent flow [50]. The parameter σ_ε is a "Prandtl" number for ε and values for the constants are taken as $C_1 = 1.44$ $C_2 = 1.92$ and $\sigma_\varepsilon = \kappa^2/[(C_2 - C_1)C_\mu{}^{1/2}]$ from [50]. Term A_3 in Eq. (18) represents a proportion of ε which is apportioned to the particulate phase due to direct dissipation of k by fluid-particle interaction effects. The term has been modeled in [49] where it is shown that:

$$A_3 = \varepsilon - \nu\left[\frac{\varepsilon}{\nu}\frac{T_L}{\tau_m+T_L} + \frac{\tau_m}{(\tau_m+T_L)^2}\frac{\partial k}{\partial x_j}\frac{\partial T_L}{\partial x_j}\right] \tag{19}$$

This expression yields $A_3 \to 0$ for $\tau_m/T_L \to 0$, meaning that for short response times fluid-particle interactions result in negligible direct dissipation of fluid turbulent kinetic energy by the particulate phase.

Equations (1, 2, 8, 13, 15, 17, and 18) constitute a set of 7 equations from which to solve for the unknowns: U_{f_i}, U_{p_i}, α, P, k, ε, k_p. To achieve this, use must be made of the additional relations given by Equations (3, 9, 12, 14, 16, and 19), and appropriate boundary conditions must be specified.

2.3 Boundary Conditions

a) Fluid Phase

At either channel wall the shear stress for the fluid phase is prescribed from the universal law of the wall distribution for velocity [50]. This empirical function relates the wall stress to the tangential velocity component calculated at the nodes nearest the wall. The normal velocity component at the wall is set equal to zero. The entrance velocity distribution is presumed known or taken from experiments. The exit boundary condition for velocity is also presumed known or, in the event of being unavailable, a fully developed flow condition is set by specifying the following streamwise condition:

$$\left.\frac{\partial \phi}{\partial x}\right|_{\text{exit plane}} = 0 \tag{20}$$

where $\phi = U_{f_i}$. The effect of particles on the law of the wall distribution for velocity have been shown to be significant for non-dilute, inertial particle systems [31, 51, 52]. Only for inter-particle distances larger than the scale of the energy containing eddies do Peskin and Dwyer [31] show a negligible influence of the particle phase. This condition is presumed to arise in the present work but requires further analysis for rigorous justification.

The specification of k at the channel walls is accomplished by assuming local equilibrium of the flow in the wall region [50]. Analysis given in [49] of laser-Doppler measurements of turbulent shear stress made by Zisselmar and Molerus [32] suggests that for systems with $\alpha < 0.035$ and values of τ_m of interest to this work, the particulate phase does not alter strongly the distribution of k in the near wall region. The transport equation for k then yields an expression for k in terms of the wall stress. The inlet value of k is presumed known, or taken from experiment. The exit plane value is taken from experiment or fixed by specifying $\phi = k$ in Eq. (20).

Wall values of ε are determined by requiring that the turbulence length scale vary linearly with distance from the wall [50]. Substitution of the gradient of velocity from the law of the wall into the simplified (near-wall region) turbulent kinetic energy balance yields the necessary relation for ε [50]. As for k, particle effects on the distribution of ε near a wall are shown in [49] to be small. The exit plane distributions for ε is dealt with as for k. At the inlet plane ε is specified from:

$$\varepsilon = \frac{k^{3/2}\big|_{inlet}}{0.01\ D} \tag{21}$$

where D is the channel width or pipe diameter.

b) <u>Particulate Phase</u>

The wall shear stress and the slip velocity for the particulate phase can be found from the relations derived by Stuckel and Soo [34] and Soo [27]. These are:

$$(\tau_p)_w = \frac{1}{2\sqrt{\pi}} (\rho_p)_w \ (U_p)_w \ (\tfrac{2}{3} k_p)_w^{1/2} \tag{22}$$

and

$$(U_p)_w = \tau_m \left[\frac{2}{3}(k+k_p) - 2k\left(\frac{T_L}{\tau_m+T_L}\right)\right]^{1/2} \left(\frac{\partial U_p}{\partial n}\right)_w \tag{23}$$

where n is the coordinate direction normal to a wall. Particle inertial effects associated with acceleration of the fluid phase over a short entrance length in the channel are neglected in Eq. (23), but are available in [49]. The particulate phase velocity component normal to a wall was set equal to zero.

The treatment for the particulate phase velocity components at the entrance and exit planes are the same as those described above for the fluid phase.

Boundary condition specifications for k_p follow directly from Eq. (17) and a knowledge of the distribution for k.

The boundary conditions for α at a wall were prescribed to conform with an impermeable wall condition:

$$\left.\frac{\partial \alpha}{\partial n}\right|_{wall} = 0 \tag{24}$$

Inlet and exit plane boundary conditions for α were prescribed as for velocity.

2.4 The Erosion Model

The problem of surface wear by particle impingement has been reviewed recently by Tilly [53]. The author discusses mechanisms of erosion and clarifies the roles played by the various contributing factors. Among the most important parameters affecting particle impingement erosion are: particle shape, size, density, concentration and hardness; the particle impact velocity and angle of attack with respect to the surface; conditions at the eroded surface such as roughness, duration of exposure and physical properties of the surface.

Tilly [53] discusses the relative merits of the ductile metal surface-gas-solid particle erosion model proposed by Finnie [54]. In the model the cutting action of solid particles is assumed to be similar to that of cutting tools, with the cutting depth depending on the surface material physical properties. Because this model shows good agreement with experimental data for shallow angles of attack, and because it is relatively simple to implement, it was used for this study. The volume rate of removal of wall material per unit surface area predicted by this model is given by:

$$\dot{E} = c \frac{\dot{m}_p}{p_1} q_p^2 f(\beta) \tag{25}$$

In Eq. (25) the variables are defined as:

$\dot{E}$ erosion rate in terms of volume per unit area and time

c fraction of the number of particles cutting in an idealized manner

p_1 Vickers hardness of the wall material

$\dot{m}_p$ particle mass striking the surface per unit area and unit time

q_p the magnitude of the particulate phase impact velocity

$f(\beta)$ function of particle angle of attack, β (measured with respect to the wall)

The following expressions for $f(\beta)$ arise:

$$\begin{aligned} f(\beta) &= \sin(2\beta) - 4\sin^2\beta & \beta &\leq 14° \\ f(\beta) &= \cos^2\beta/4 & \beta &> 14° \end{aligned} \tag{26}$$

2.5 The Solution Algorithm

The basis for the numerical algorithm used to solve finite difference forms of the equatins presented in section 2.2 is the TEACH code. This type of numerical procedure has been used extensively for predicting laminar and turbulent flows and has already been described and extensively documented in various communcations. Among the most informative of these are [55-59]. The procedure was extended as described in [49] to accommodate the presence of a solid phase in the flow.

The forms of the finite difference equations for the two phases were obtained in the same way as described in the references. Variables were solved iteratively on a staggered interconnected calculation grid. A solution was obtained when the maximum normalized value of any of the residual sources for momentum or mass was less than 10^{-3}. Under-relaxation factors for velocity were set equal to 0.5 and for pressure equal to 1.0.

Calculations were performed on a 20×40 grid for curved channels and on an 18×50 grid for straight channels. The grids were evenly spaced in the streamwise direction and unevenly spaced in the transverse direction. The optimum transverse spacing was determined empirically in each case. Grid refinement tests showed that while finer grids than the ones used would have improved the results, the costs involved would have outweighed the benefits. It is estimated that the results presented here are within 10% of grid-independent solutions. Typical storage and calculation time requirements on a CDC 7600 computer were 155 k_8 words, and 200 CPU seconds for 225 iterations.

3. Results and Discussion

The following two sections present the main results of this study. First, testing of the numerical model was performed and some of the results are discussed here; particularly those relating to erosion since adequate data for conducting such tests is sparse. Second, the model was applied to curved channel flows with different conditions, for which data is unavailable. Although the numerical model has performed quite satisfactorily with respect to the tests, these are few and confidence should strictly be placed only on the <u>relative</u> value of the extrapolations. Checks on the accuracy of the absolute values of the new curved channel results await the availability of appropriate experimental data.

3.1 Numerical Model Testing

Unfortunately, there are few reliable experimental investigations, with detailed enough measurements of the variables needed, for testing and evaluating the performance of fluid-solid two-phase turbulence models. A careful search revealed only four studies which could be readily and usefully employed for model testing and evaluation. These were: the straight channel studies of Stuckel and Soo [34]; the straight pipe studies of Kramer and Depew [33], and Zisselmar and Molerus [32]; and the curved duct study of Mason and Smith [60]. In their study, Zisselmar and Molerus used a laser-Doppler velocimeter to investigate the motion of dilute suspensions of glass particles in methyl benzoate, and the data provided is quite detailed. The remaining studies pertain to solid particles suspended in air. Table 1 provides a relative comparison of some of the principal characteristics of these investigations.

Figures 1-a and 1-b provide a comparison between calculated and measured values of fluid and particulate phase mean longitudinal velocities for two concentrations in the pipe flow configuration of Kramer and Depew [33]. In general, the comparison shows very good agreement, with the present model yielding superior predictions than the single-phase model of [33]. Similar profiles for the configuration of Stuckel and Soo [34] displayed the same level of agreement, although measured particulate phase velocities systematically lagged behind the predicted values by as much as 12% due to the delaying action of electrostatic forces present in the experiment which were not included in the model.

Centerline values for developing fluid and particle streamwise velocities are shown in Figures 2-a and 2-b. Again, the agreement between measurements and predictions falls well within the scatter in the data over a substantial range of the Reynolds number. The streamwise variation of the particulate-phase wall-slip velocity is shown in Figure 3. The agreement shown in the figure is an indirect confirmation of the validity of the wall treatment used for the fluid and particle phases in the present model.

Comparisons between the predicted and measured transverse variations of streamwise slip velocity, given in Figures 4-a and 4-b for the configuration of Kramer and Depew [33] show better agreement for the case of small particles (d_p = 62 μm) than for the case of large particles (d_p = 200 μm). In addition, for the small particles better predictions are shown for the more dilute flow. The deviations displayed for the cases of larger particles and higher concentrations are in keeping with the limitations embodied in the model. It is estimated in [49] that typical response times for the larger particles were ten times greater than for the small. The slip Reynolds number for the large and small particles were about 130 and 12 respectively, indicating the invalidity of assuming Stokes drag law for the larger particles. Also, in both cases particle sizes were larger than the estimated Kolmogorov length scale for the fluid phase η, which was bounded by $10 \leq \eta \leq 100$ μm in the experiment. This suggests that the assumption of a continuum, that $d_p << \eta$, is questionable, but more seriously for the larger particle case. The points just made partly explain the differences arising between the two particle sizes. Negative values of the slip velocity near the wall are due to the fluid having to come to rest at the wall while the particulate phase slips by.

The influence of average particle concentration, on the fluid turbulent kinetic energy and turbulent shear stress are shown in Figure 5 for the fully-developed straight pipe flow case of Zisselmar and Molerus [32]. Both the experiments and the calculations show that increasing α lowers k; k can be reduced by as much as 50% for α = 5.6%. The reduction in k is attributed principally to the transfer of turbulent kinetic energy from the fluid to the particulate phase; term A_2 in Eq. (15). The underprediction of k for the larger values of α is due, in part, to the breakdown of the diluteness assumption. As shown in Figure 5-c the decrease in fluid turbulent shear stress with α near the pipe wall is reproduced.

In contrast to straight channel flow, the dearth of two-phase flow experimental data in curved channels has precluded any detailed testing for this configuration. Mason and Smith [60] provide measurements of erosion in curved ducts as a function of bend angle for two curvature ratios. Although their flow is three-dimensional, two-dimensional predictions of erosion using the model of this study show good qualitative agreement with the measurements in Figure 6. The initial sharp rise in erosion rate, the location of maximum erosion and the subsequent tailing as a function of bend angle at the concave wall of the duct are faithfully reproduced. The very low values of erosion found experimentally for both curvatures between 30 and 50 degrees are not predicted. It has been shown by Humphrey, Whitelaw and Yee [61] for a similar configuration that cross-stream flows arising at these locations are in the order of 30% of the bulk average velocity through the duct. Such large lateral motions will tend to reduce the particle angle of attack, and its kinetic energy through repeated collisions with the walls, thus inducing a reduction in erosion rate.

3.2 Application to Curved Channel Flow

In this section are given the main results obtained from applying the numerical model to 90° curved channel flows of practical interest. The testing described in section 3.1 has demonstrated the adequacy of the computational model for predicting turbulent two-phase flow in confined two-dimensional configurations. Testing of the model's capability to predict erosive wear, while very encouraging, is much less complete. The results given here may be inaccurate in terms of their absolute magnitudes, particularly those relating to erosive wear. Notwithstanding, in the absence of experimental information, the relative comparisons which the predictions allow are of considerable value for purposes of design, and for helping to quantify the relative importance of the roles played by the various controlling parameters. It is with this thinking that this section should be regarded.

Fluid Mechanic Results

Calculations were made of the streamwise mean velocity components for the fluid and particulate phases in developing curved channel flow. Representative samples of some of the profiles are shown in Figure 7, with the calculated conditions indicated. The conditions correspond to a mildly curved channel containing a liquid such as water (or solvent refined coal) with particles such as sand (or coal) in suspension. The inlet flow to the curved channel was specified as being fully developed straight channel flow. Calculations performed with $\alpha = 0.1$ and $\psi = 0.01$ did not differ significantly from the results shown in Figure 7-a, while predictions performed with $\alpha = 0.001$ and $\psi = 100$ were very similar to the results given in Figure 7-b. The dimensionless particle response time parameter shown in these and subsequent figures is defined as:

$$\psi \equiv \tau_m U_{fo}/\Delta \tag{27}$$

with the particle response time τ_m given by Eq. (6); Δ being the channel width; and U_{fo} being the average fluid velocity at the channel inlet. As shown in the figures, slip velocity between the two phases becomes significant for $\psi \geq 1$, is large for $\psi = 100$, and is an increasing function with bend angle. For large values of ψ the Coriolis force acting on the particulate phase has the effect of decelerating particles at the concave wall ($y/\Delta = 1$) relative to the convex ($y/\Delta = 0$). The calculations revealed that particle slip velocity was independent of concentration for all cases with $\alpha < 0.1$.

The fluid-particulate phase vector velocity plots shown in Figure 8 help visualize the calculation conditions discussed above. In the plots, of any pair of vectors at a point, the one pointing more directly to the concave wall corresponds to the solid phase. For $\psi = 100$ it is seen clearly that particles strike the concave wall of the channel at an acute angle to the fluid streamlines.

The transverse variation of fluid turbulent kinetic energy is shown in Figure 9 for fully developed curved channel flow. The plots indicate that decreasing ψ and increasing α both lead to decreasing k in the flow. These predictions are in agreement with the turbulent kinetic energy exchange mechanisms discussed in section 2.2. Corresponding plots of the particulate phase turbulent kinetic energy are given in Figure 10. The relative influence of the response time parameter is now reversed, with the figures showing that sluggish particles ($\psi > 1$) have a smaller proportional amount of turbulent kinetic energy. The role of α in both cases is the same, increasing the particle concentration dampens the turbulent kinetic energy component of both phases in the flow. The peaks displayed by the k_p profiles for $\psi = 1$ and 100 are due to the modulating effect that the time scale ratio τ_m/T_L has on k; see Eq. (17). From Eq. (6) and (7) this ratio is seen to be proportional to $(k/\varepsilon)^{-1}$.

Erosive Wear Results

Erosive wear at the concave wall of a curved channel was predicted as a function of channel angle for different values of the particulate phase response time parameter, ψ, and channel flow Reynolds number, Re. The particle/fluid density ratio was 1.8. The results were plotted in the form of "erosion maps" a sequence of which is given in Fig. 11. The maps show that sluggish particle ($\psi > 1$) tend to produce significant wear at all flow speeds. Responsive particles are more erosive at the higher flow speeds, but their rate of wear is typically $10^2 - 10^5$ times less than that of the sluggish particles. From the maps it is also seen that for fixed Re the position of maximum wear moves downstream with increasing ψ, as should be anticipated.

The wear profiles show that for $\theta \geq 70°$ the rate of erosion is essentially constant. Then, for a fixed ψ and Re:

$$\dot{E} \propto [\alpha\ U_P^2]_{inlet} \tag{28}$$

The form of this relation has also been derived by Laitone [17] and by Yeung [62].

A simple force balance for responsive particles ($\psi < 1$) shows [49] that the particle angle of impingement at the concave wall in curved channel flow is given by:

$$\beta \lesssim \tan^{-1} (\psi \frac{\Delta}{r}) \tag{29}$$

where r is the radial location of a point in the channel. It is seen that, for example, with $R_c/\Delta = 12$, $\psi \approx 10^{-5}$, using 5 μm solid particles with $\tilde{\rho}_p/\tilde{\rho}_f = 1.8$, the impingement angle is $\beta \approx 10^{-4}$ and is too small to cause significant erosion even at high speeds.

In addition to the results given here, values for the streamwise variation of particulate phase kinetic energy and angle of attack upon impact with the wall, have been calculated and are available in [49].

4. Conclusions

This study has been performed to advance present-state turbulence modeling concepts relating to two-phase flow, with the aim of developing and applying a computational model capable of predicting such flows and related erosion phenomena.

Analysis shows that viscous interactions between the fluid and particulate phases cause reductions in the turbulent kinetic energy of both. The mechanisms of kinetic energy exchange involve transport: a) from the turbulent kinetic energy of the fluid to the turbulent kinetic energy of the particulate phase; b) from the mean kinetic energy of the fluid to the turbulent kinetic energy of the particulate phase <u>via</u> the turbulent kinetic energy of the fluid.

In general, predictions based on the present model are in good agreement with available two-phase flow data. Deviations between measurements and calculations arise for $\alpha > 0.05$, $Re_p > 1$, $\psi >> 1$, and when large field forces exist in the experiments. In spite of its limitations, the model faithfully represents all the important features arising in connection with two-phase flows.

It is shown how the use of a relatively simply expression for erosive wear permits application of the model for predicting erosion in curved channel flow. In this regard relative trends are also faithfully represented by the calculation procedure.

Further testing of the computational model is required and is the subject of continued research by one of us (JACH) in the context of three-dimensional curved duct flow. For this purpose, the program of research includes laser-Doppler measurements of the fluid and particulate phase velocities and corresponding turbulence characteristics. Emphasis will be placed on relieving the diluteness assumption and extending the theoretical base for dealing with flows in which $\alpha > 0.1$. The inclusion of field forces is also of interest and will be incorporated.

Although there are numerous practical research activities in the field of fluid-particulate turbulent flows, detailed fundamental investigations remain an absolute necessity. In particular, there is a serious need for quantitative experimental work yielding accurate results of value for guiding and testing numerical models for these flows. Strategically planned, carefully executed, fundamental experimental work will continue to play a dominant role in future theoretical and modeling advancements relating to turbulent two-phase flows.

Acknowledgements

This study was made possible by the Technical Coordination Staff of the Office of Fossil Energy of the U.S. Department of Energy, under Contract No. DE-AC03-76SF00098 through the Fossil Energy Materials Program, Oakridge National Laboratory, Oakridge, Tennessee. The authors also wish to express their appreciation to Mrs. Judy Reed for the fine typing of this difficult manuscript.

References

[1] Soo, S. L. Fluid dynamics of multiphase systems. Blaisdell Publishing Co., Waltham, Massachusetts, 1967.

[2] Boothroyd, R. G. Flowing gas-solids suspensions. Chapman and Hall Ltd., London, England, 1971.

[3] Torobin, L. B. and Gauvin, W. H. Fundamental aspects of solids-gas flow. Can. J. Chem. Eng., 37, p. 129, 167, 224, 1959.

[4] Torobin, L. B. and Gauvin, W. H. Fundamental aspects of solids-gas flow. Can. J. Chem. Eng., 38, p. 142, 189, 1960.

[5] Torobin, L. B. and Gauvin, W. H. Fundamental aspects of solids-gas flow. Can. J. Chem. Eng., 39, p. 113, 1961.

[6] Soo, S. L. Non-equilibrium fluid dynamics-laminar flow over a flat plate. ZAMP, 19, pp. 545-563, 1968.

[7] Drew, D. A. Two phase flows: constitutive equations for lift and Brownian motion and some basic flows. Archive for Rational Mechanics and Analysis, 62, no. 2, pp. 149-163, 1976.

[8] Hinze, J. O. Momentum and mechanical energy balance equations for a flowing homogeneous suspension with slip between the two phases. Appl. Sci. Res., 11, section A, pp. 33-46, 1972

[9] Hinze, J. O. Turbulent fluid and particle interactions. Prog. in Heat and Mass Transfer, 6, Pergamon Press, New York, pp. 433-452, 1972.

[10] Drew, D. A. Production and dissipation of energy in the turbulent flow of a particle-fluid mixture, with some results on drag reduction. J. Appl. Mech. Trans. ASME, no. 4, pp. 543-547, 1976.

[11] Nagarajan, M. On the turbulent pipe flow of gas-solids suspensions. Aerosol Sci., 3, pp. 157-165, 1972.

[12] Soo, S. L. Fully developed turbulent pipe flow of a gas-solid suspension. Ind. and Eng. Chem. Fundamentals, 1, no. 1, pp. 33-37, 1962.

[13] Wallis, G. B. One-dimensional two-phase flow. McGraw-Hill, New York, 1969.

[14] Glauert, M. A method of constructing the paths of raindrops of different diameters moving in the neighborhood of (1) a circular cylinder, (2) an aerofoil, placed in a uniform stream of air; and a determination of the rate of deposit of the drops on the surface and the percentage of drops caught. R&M, British A.R.C. no. 2025, 1940.

[15] Langmuir, I. and Blodgett, K. B. A mathematical investigation of water droplet trajectories. Tech. Rep. No. 5418, Air Material Command, AAF, 1946.

[16] Brun, R. J. and Mergler, H. W. Impingement of water droplets on a cylinder in an incompressible flow field and evaluation or rotating multicylinder method for measurement of droplet-size distribution, volume-median droplet size, and liquid-water content in clouds. NACA TN 2904, 1973.

[17] Laitone, J. A. Separation effects in gas-particle flows at high Reynolds numbers. Ph.D. thesis, University of California, Berkeley, 1979.

[18] Yeung, W. S. Fundamentals of the particulate phase in a gas-solid mixture. Lawrence Berkeley Laboratory, Berkeley, California, Report No. LBL-8440, 1978.

[19] Abuaf, N. and Gutfinger, C. Trajectories of charged solid particles in an air jet under the influence of an electrostatic field. International Journal of Multiphase Flow, 1, pp. 513-523, 1974.

[20] Baw, P. S. and Peskin, R. L. Some aspects of gas-solid suspension turbulence. Trans. ASME, J. Basic Eng., 93D, pp. 631-635, 1971.

[21] Owen, P. R. Pneumatic transport. J. Fluid Mech., 39, part 2, pp. 407-432, 1969.

[22] Soo, S. L., Ihrig, Jr., H. K. and El Kough, A. F. Experimental determination of statistical properties of two-phase turbulent motion, J. Basic Eng., Trans. ASME, 82D, no. 3, pp. 609-621, 1960.

[23] Kada, J. and Hanratty, T. J. Effects of solids in turbulence in a fluid. A.I.Ch.E. Jour., 6, no. 4, pp. 624-630, 1960.

[24] Hino, M. Turbulent flow with suspended particles. Proc. ASCE Journal, J. Hydr. Div., HY4, pp. 161-187, 1963.

[25] Peskin, R. L. Some fundamental research problems in gas-solids flows. Am. Inst. of Chem. Eng. Symposium Series, 71, no. 147, pp. 42-59, 1975.

[26] Soo, S. L. Boundary layer motion of a gas-solids suspension. Proceedings of Symposium on 'Interactions Between Fluids and Particles'. Institute of Chemical Engineers, London, pp. 50-63, 1962.

[27] Soo, S. L. Pipe flow of suspensions. Appl. Sci. Res., 21, pp. 68-84, 1969.

[28] Soo, S. L. Pipe flow of suspensions in turbulent fluid. Electrostatic and gravity effects. Appl. Sci. Res., 24, pp. 83-97, 1971.

[29] Peskin, R. L. Some effects of particle-particle and particle-fluid interactions in two-phase flow systems. Ph.D. thesis, Princeton University, Princeton, New Jersey, 1959.

[30] Peskin, R. L. The diffusivity of small suspended particles in turbulent fluids. Presented at the National Meeting A.I.Ch.E., Baltimore, Maryland, 1962.

[31] Peskin, R. L. and Dwyer, H. A. Study of mechanis of turbulent gas-solid shear flows. ASME, paper no. 65-WA/FE-24, 1965.

[32] Zisselmar, R. and Molerus, O. Investigations of solid-liquid pipe flow with regard to turbulence modification. Chem. Eng. J., 18, pp. 233-239, 1979.

[33] Kramer, T. J. and Depew, C. A. Experimentally determined mean flow characteristics of gas-solid suspensions. ASME, paper no. 72-FE-29, 1972.

[34] Stukel, J. J. and Soo, S. L. Turbulent flow of a suspension into a channel. Powder Technology, 2, pp. 278-289, 1969.

[35] Soo, S. L. and Trezek, G. J. Turbulent pipe flow of magnesia particles in air. Ind. and Eng. Chem. Fundamentals, 5, no. 3, pp. 388-392, 1966.

[36] Soo, S. L. and Regalbuto, J. A. Concentration distribution in two-phase pipe flow. Can. J. of Chem. Eng., 38, no. 5, pp. 160-166, 1960.

[37] Soo, S. L. and Tung, S. K. Deposition and entrainment in pipe flow of a suspension. Powder Technology, 6, pp. 283-295, 1972.

[38] McCarthy, H. E. and Olson, J. H. Turbulent flow of gas-solids suspensions. Ind. and Eng. Chem. Fund., 5, no. 3, pp. 417-477, 1968.

[39] Reddy, K. V. S. and Pei, D. C. T. Particle dynamics in solid-gas flow in a vertical pipe. Ind. Eng. Chem. Fund., 8, no. 3, pp. 490-497, 1969.

[40] Drew, D. A. Turbulent sediment over a flat bottom using momentum balance. J. Appl. Trans. ASME, 97E, pp. 38-44, 1975.

[41] Nagarajan, M. and Murgatroyd, W. A simple model of turbulent glass-solids flow in a pipe. Aerosol Sci., 2, pp. 15-22, 1971.

[42] Kramer, T. J. and Depew, C. A. Analysis of mean flow characteristics of gas-solids suspensions. J. Basic Eng. Trans. ASME, 94D, pp. 731-738, 1972.

[43] Yuu, S., Yasukouchi, N., Hirosawa, Y. and Jotaki, T., Particle turbulent diffusion in a dust laden jet. A.I.Ch.E. Journal, 24, no. 3, pp. 409-519, 1978.

[44] Smith, P. J., Fletcher, T. H. and Smoot, L. D. Two-dimensional model for pulverized coal combustion and gasification. Meeting of the Combustion Institute, Western States Section, University of California at Irvine, pp. 21-22, 1980.

[45] Danon, H., Wolfshtein, M., Hetsroni, G. Numerical calculations of two-phase turbulent round jet. International Journal of Multiphase Flow, 3, pp. 223-234, 1977.

[46] Genchev, Zh. D. and Karpuzov, D. S. Effects of the motion of dust particles on turbulence transport equations. J. Fluid Mech., 101, part 4, pp. 833-842, 1980.

[47] Harlow, F. H. and Nakayama, P. I. Turbulence transport equations. Phys. of Fluids, 10, no. 11, pp. 2323-2332, 1967.

[48] Launder, B. E. and Spalding, D. B. The numerical computation of turbulent flows. Comput. Meths. Appl. Mech. Engrg., 3, p. 269, 1974.

[49] Pourahmadi, F. Turbulence modeling of single and two phase curved channel flows. Ph.D. thesis, University of California, Berkeley, 1982. Also available as Lawrence Berkeley Laboratory Report No. LBL-13808.

[50] Humphrey, J. A. C. and Pourahmadi, F. A generalized algebraic relation for predicting developing curved channel flow with a k-ε model of turbulence, LBL Report No. 12009, Lawrence Berkeley Laboratory, University of California, 1981.

[51] Davidson, G. A. and McComb, W. D. Turbulent diffusion in an aerosol jet. J. Aerosol Sci., 6, pp. 227-247, 1975.

[52] Wells, Jr. C. S., Harkness, J. and Meyer, W. A. Turbulence measurements in pipe flow of a drag-reducing non-Newtonian fluid. AIAA J., 6, no. 2, pp. 250-257, 1968.

[53] Tilly, G. P. Erosion caused by impact of solid particles. Treatise on Materials Science and Technology, Vol. 13, pp. 287-319. Academic Press, 1979.

[54] Finnie, I. Some observations on the erosion of ductile metals, Wear, 19, pp. 81-90, 1972.

[55] Gosman, A. D. and Pun, W. M. Calculation of recirculating flows. (lecture notes). Department of Mechanical Engineering, Imperial College, London, Rep. No. HTS/74/2, 1974.

[56] Patankar, S. V. and Spalding, D. B. A calculation procedure for heat, mass and momentum transfer in three-dimensional parabolic flows. Int. J. Heat and Mass Transfer, 15, pp. 1787-1806, 1972.

[57] Spalding, D. B. A novel finite difference formulation for differential expressions involving both first and second derivatives. Int. J. Num. Methods in Eng., 4, pp. 551-559, 1972.

[58] Humphrey, J. A. C. Numerical calculation of developing laminar flow in pipe of arbitrary curvature radius. Can. J. Chem. Eng., 56, p. 151, 1978.

[59] Patankar, S. V. Numerical Heat Transfer and Fluid Flow. Hemisphere Publishing Co., Washington, 1980.

[60] Mason, J. S. and Smith, B. V. The erosion of bends by pneumatically conveyed suspensions of abrasive particles. Powder Technology, 6, pp. 323-335, 1972.

[61] Humphrey, J. A. C., Whitelaw, J. H. and Yee, G. Turbulent flow strong curvature. J. Fluid Mech., 103, pp. 443-463, 1981.

[62] Yeung, W. S. Erosion in a curved pipe. Lawrence Berkeley Laboratory, Berkeley, California, Report No. LBL-7354, 1977.

Notation

C_1, C_2	constants in Eq. (18)
C_T	constant in Eq. (7)
C_μ	constant in Eq. (10)
D	pipe diameter
d_p	particle diameter
$\dot{E}$	erosion rate given by Eq. (25)
$f(\beta)$	function defined in Eq. (26)
k	fluid phase turbulent kinetic energy
k_p	particulate phase turbulent kinetic energy
$\dot{m}_p$	particle flux at a surface
n	coordinate direction normal to wall
p_1	wall Vickers hardness
P	mean pressure
q_p	magnitude of particle impingement velocity
R	straight pipe radius
R_c	curved channel radius of curvature
Re	flow Reynolds number
Re_p	particle Reynolds number
T_L	integral time scale for fluid phase (Lagrangian)
U_{f_i}	fluid phase mean velocity in i direction
U_{p_i}	particulate phase mean velocity in i direction
u_{f_i}	fluid phase velocity fluctuation in i direction
u_{p_i}	particulate phase velocity fluctuation in i direction
x_i	spatial coordinate in i direction
y	distance from pipe/channel wall

Greek letters

α	average particulate phase volume concentration
α'	fluctuating particulate phase volume concentration
β	particle impingement angle at a wall
Δ	channel width
δ_{ij}	Kronecker delta

ε dissipation rate of fluid turbulent kinetic energy
η Kolmogorov length scale
κ Von Karman constant
μ fluid phase dynamic viscosity
ν fluid phase kinematic viscosity
ν_{t_f} fluid phase turbulent viscosity
ν_{t_p} particulate phase turbulent viscosity
$\nu_{t\alpha}$ turbulent diffusivity for the transport of scalar α
ρ_p mass concentration of particulate phase
$\tilde{\rho}_f$ fluid density
$\tilde{\rho}_p$ particle density
σ_k k-Prandtl number
σ_ε ε-Prandtl number
τ_m particle response time
ϕ dummy variable in Eq. (20)
ψ dimensionless particle response time parameter defined by Eq. (27)

<u>subscripts</u>

c centerline value
f fluid phase
in. inlet value
max maximum value
p particulate phase
r radial direction in straight pipe; transverse direction in curved channel
w wall value
x streamwise direction in straight channel
z streamwise direction in straight pipe
θ streamwise direction in curved channel

Table 1

Investigators	Configuration	Re	Two-Phase System	d_p (μm)	$\frac{\tilde{\rho}_p}{\tilde{\rho}_f}$	$\alpha\|_{inlet}$
Zisselmar and Molerus [32]	straight pipe	10^5	glass particles/ methyl benzoate	53	2.51	$\leqslant 5.6\times10^{-2}$
Kramer and Depew [33]	straight pipe	$5,670-5\times10^4$	glass particles/ air	62 200	2.2×10^3	$\leqslant 4.2\times10^{-3}$
Stukel and Soo [34]	straight channel	13,000-69,800	magnesia particles/ air	14	1.4×10^3	$\leqslant 6.9\times10^{-5}$
Mason and Smith [60]	curved duct	$96\times10^3-140\times10^3$	alumina particles/ air	55	2.1×10^3	$\leqslant 2.5\times10^{-3}$

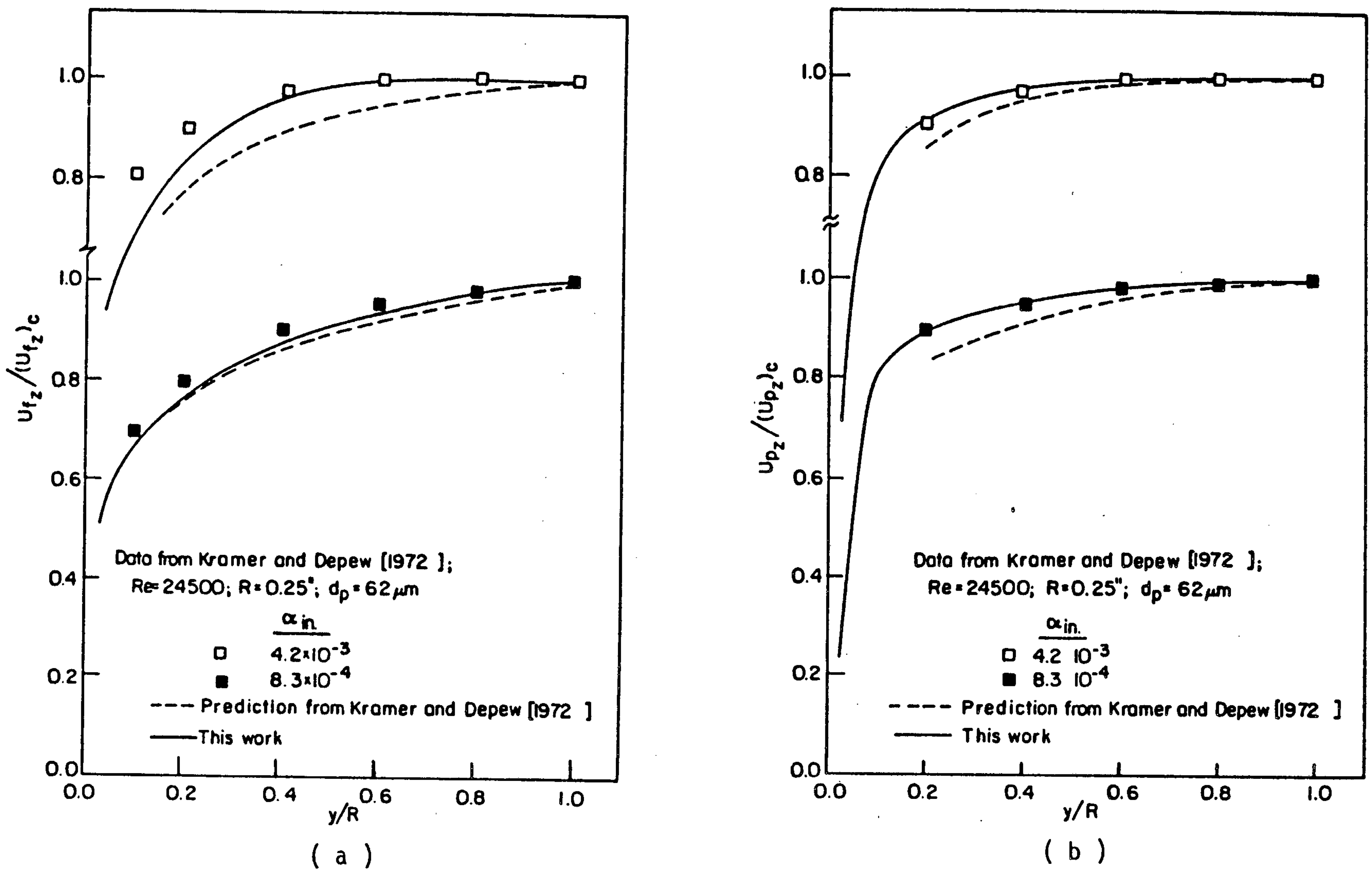

Figure 1 Transverse variation of fluid (a) and particle (b) streamwise mean velocity for two values of α at the inlet of a straight pipe flow. Velocities at pipe center used for normalization.

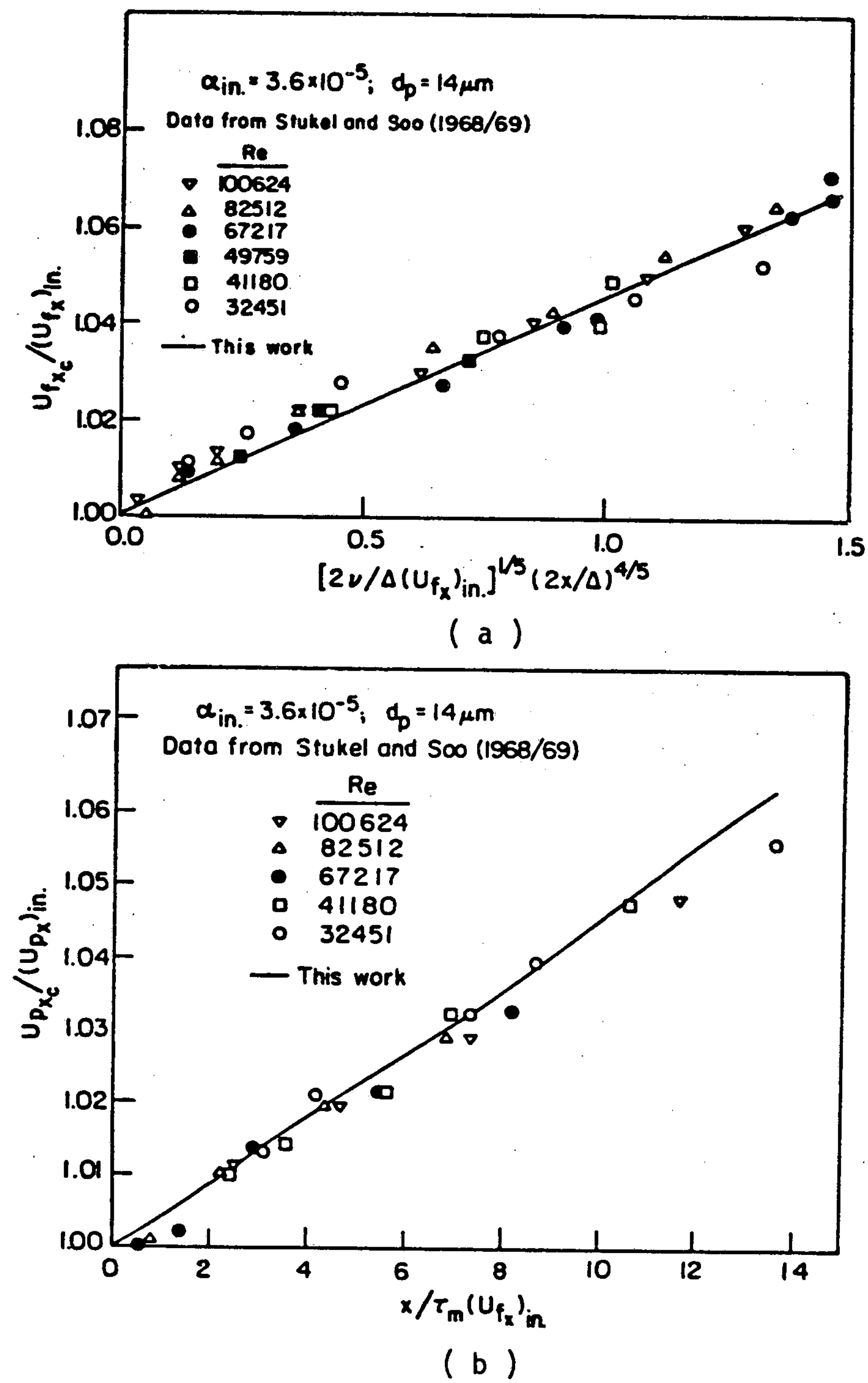

Figure 2 Streamwise variation of centerline fluid (a) and particle (b) mean velocity for developing straight channel flow. Inlet velocities used for normalization and Δ represents channel width. Streamwise location normalized following practice in [34].

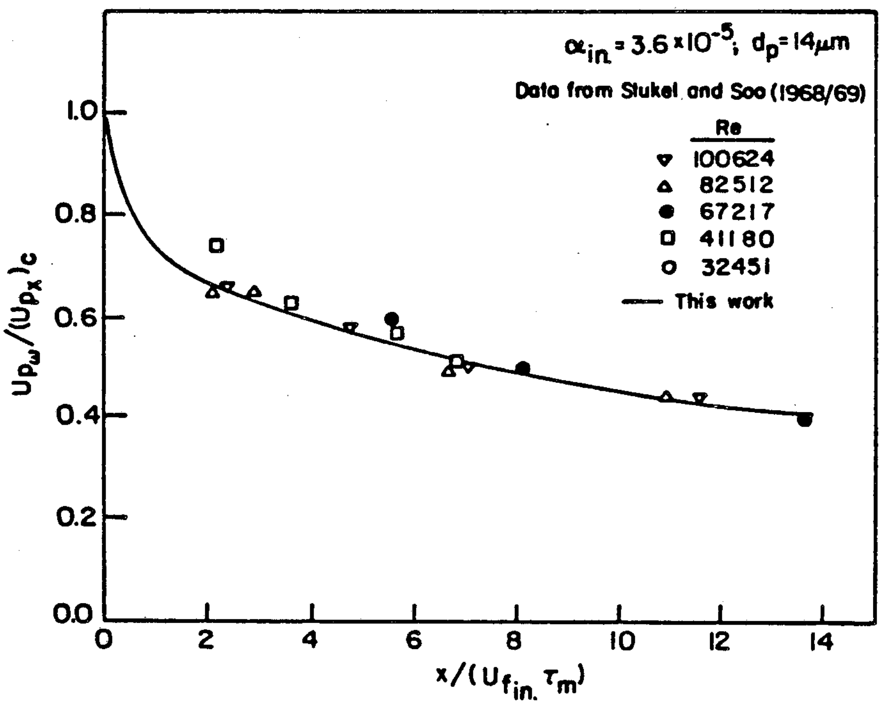

Figure 3 Streamwise variation of particulate phase wall-slip velocity in developing straight channel flow. Velocity at channel center used for normalization.

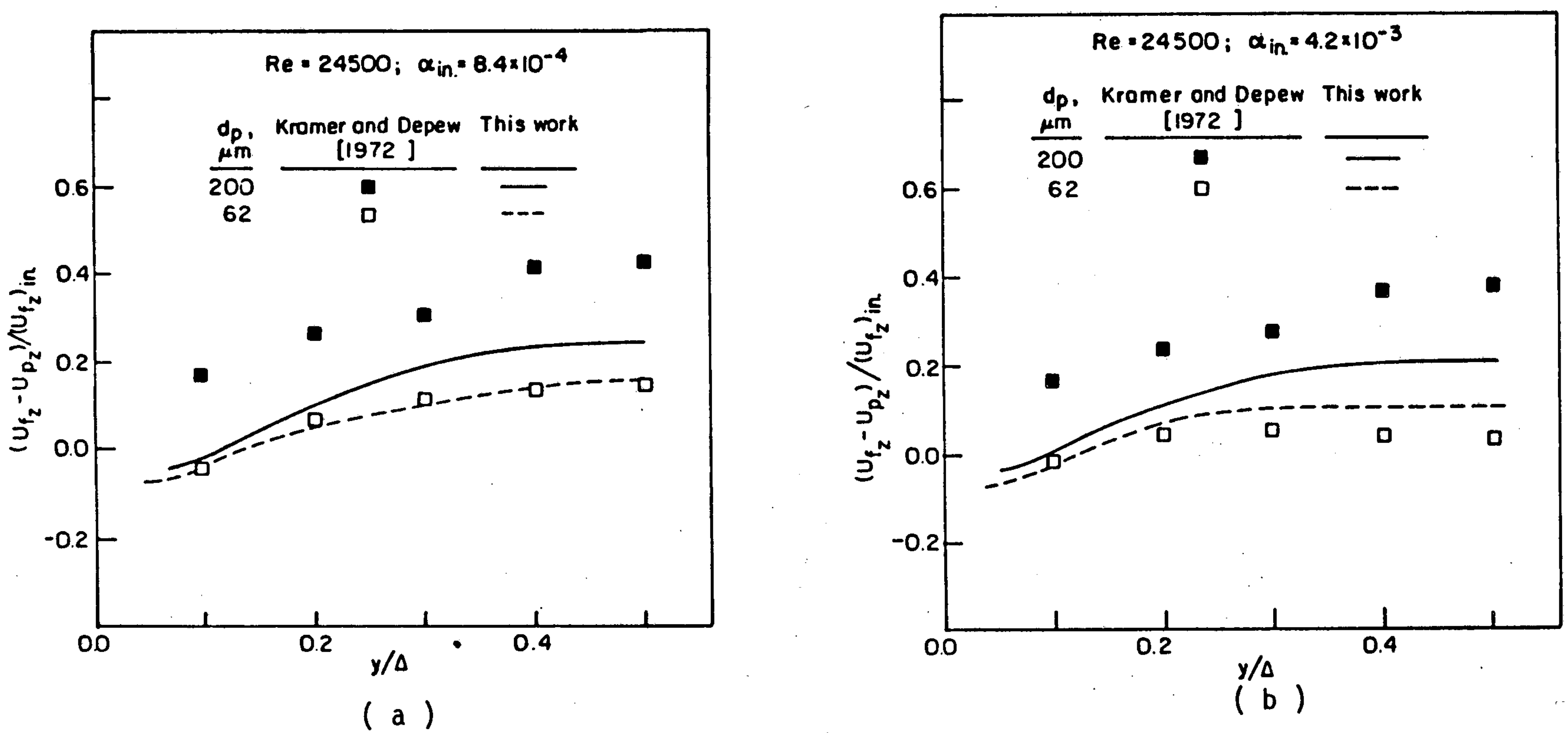

Figure 4 Transverse variation of mean slip velocity for two particle sizes and two values of α in straight pipe flow. Inlet velocity used for normalization and Δ represents channel diameter.

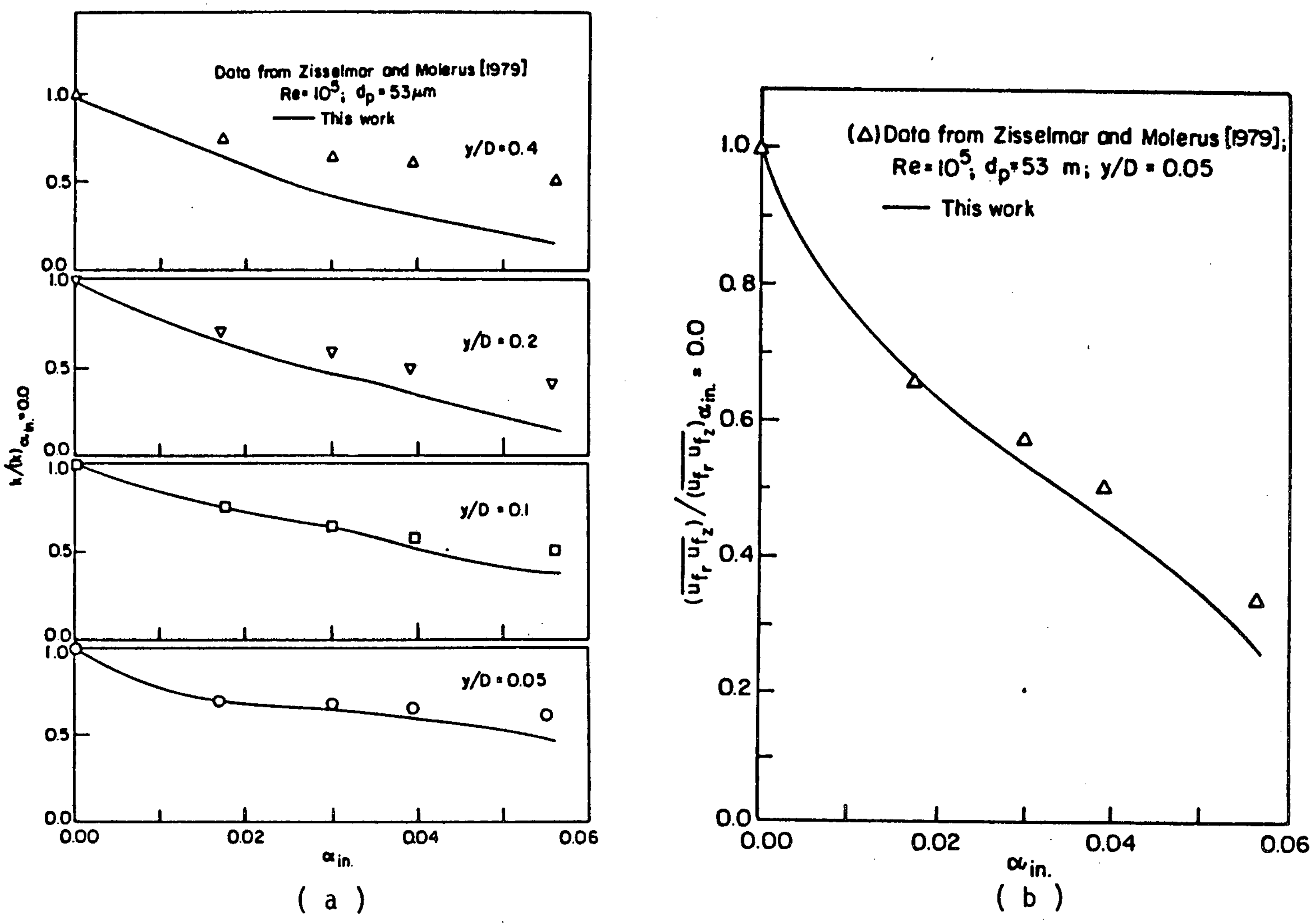

Figure 5 Effect of particulate mean volume concentration on fluid turbulent kinetic energy (a) and turbulent shear stress (b) in fully-developed straight pipe flow. Inlet values with $\alpha_{in} = 0$ used for normalization.

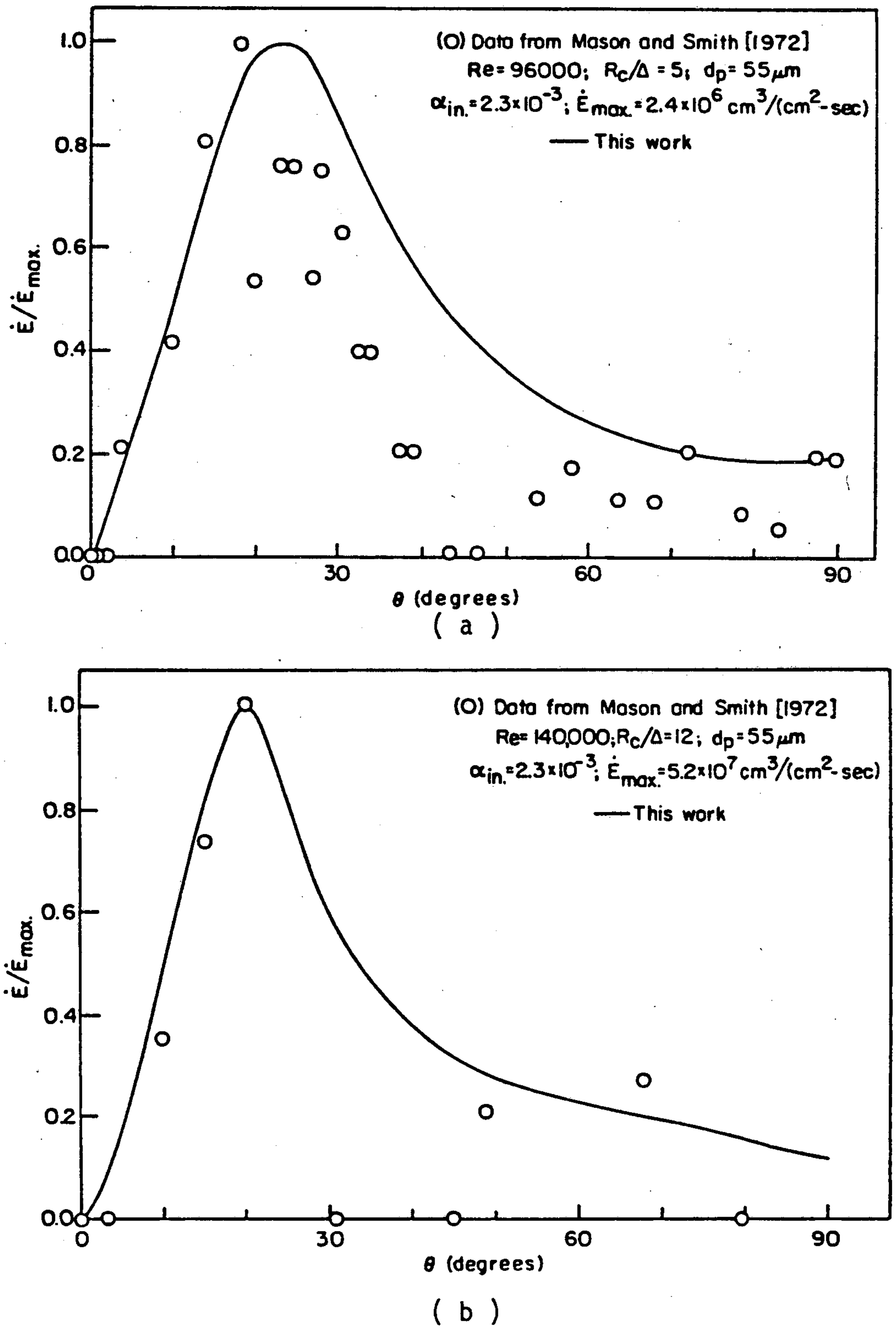

Figure 6 Two-dimensional prediction of the rate of erosion at the concave wall of a three-dimensional curved duct flow: (a) strong curvature; (b) mild curvature.

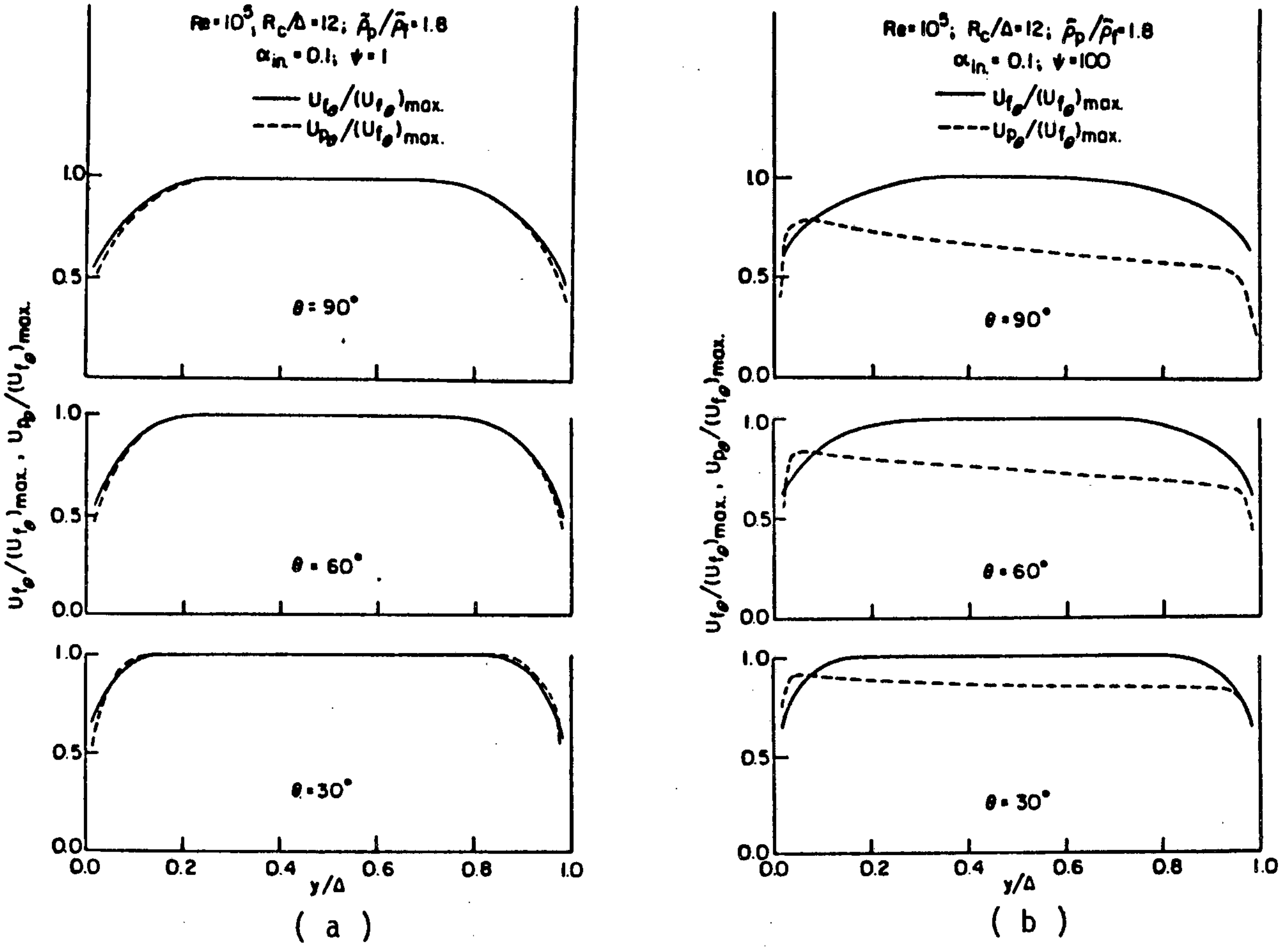

Figure 7 Transverse variation of fluid and particulate phase longitudinal mean velocity at different longitudinal positions in curved channel flow: (a) $\psi = 1$, short response time; (b) $\psi = 100$, long response time. $y/\Delta = 0$ corresponds to concave wall.

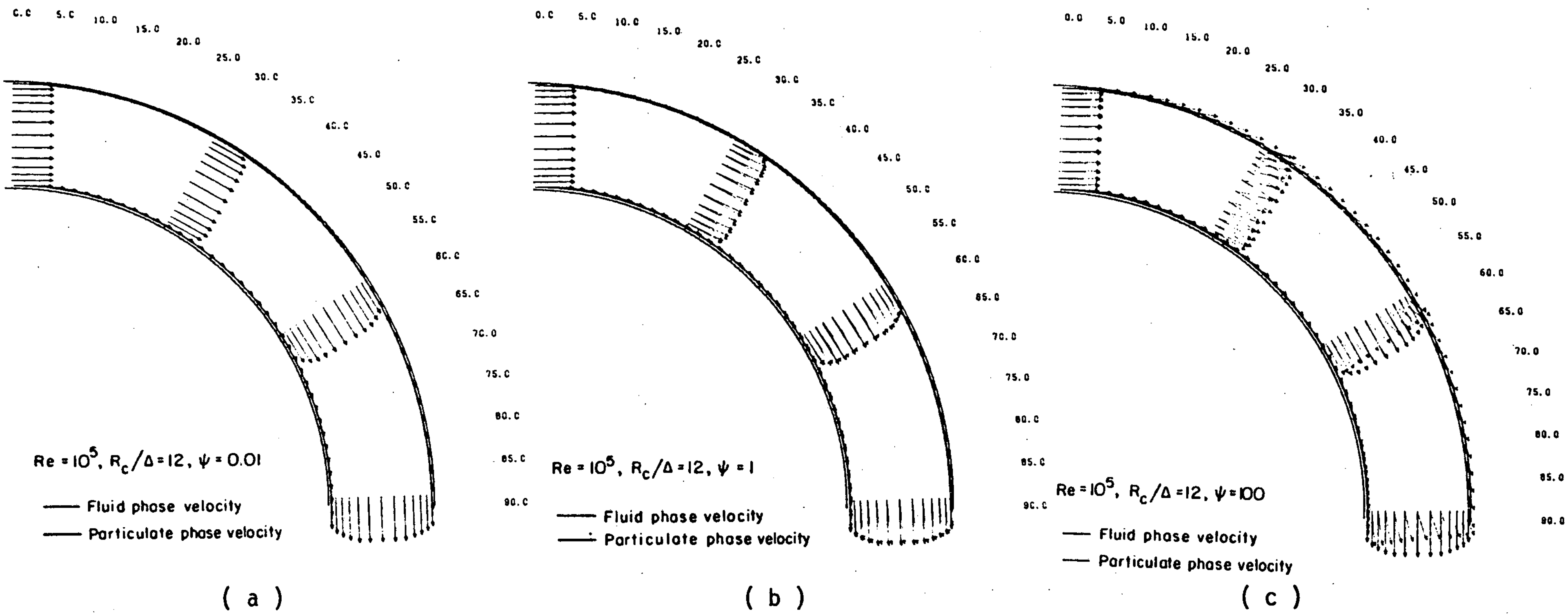

Figure 8 Vector velocity plots for the fluid and particulate phases in developing curved channel flow with $\alpha = 0.1$. The particulate phase vectors depart from the fluid phase vectors with increasing ψ and θ, and point more directly at the concave wall.

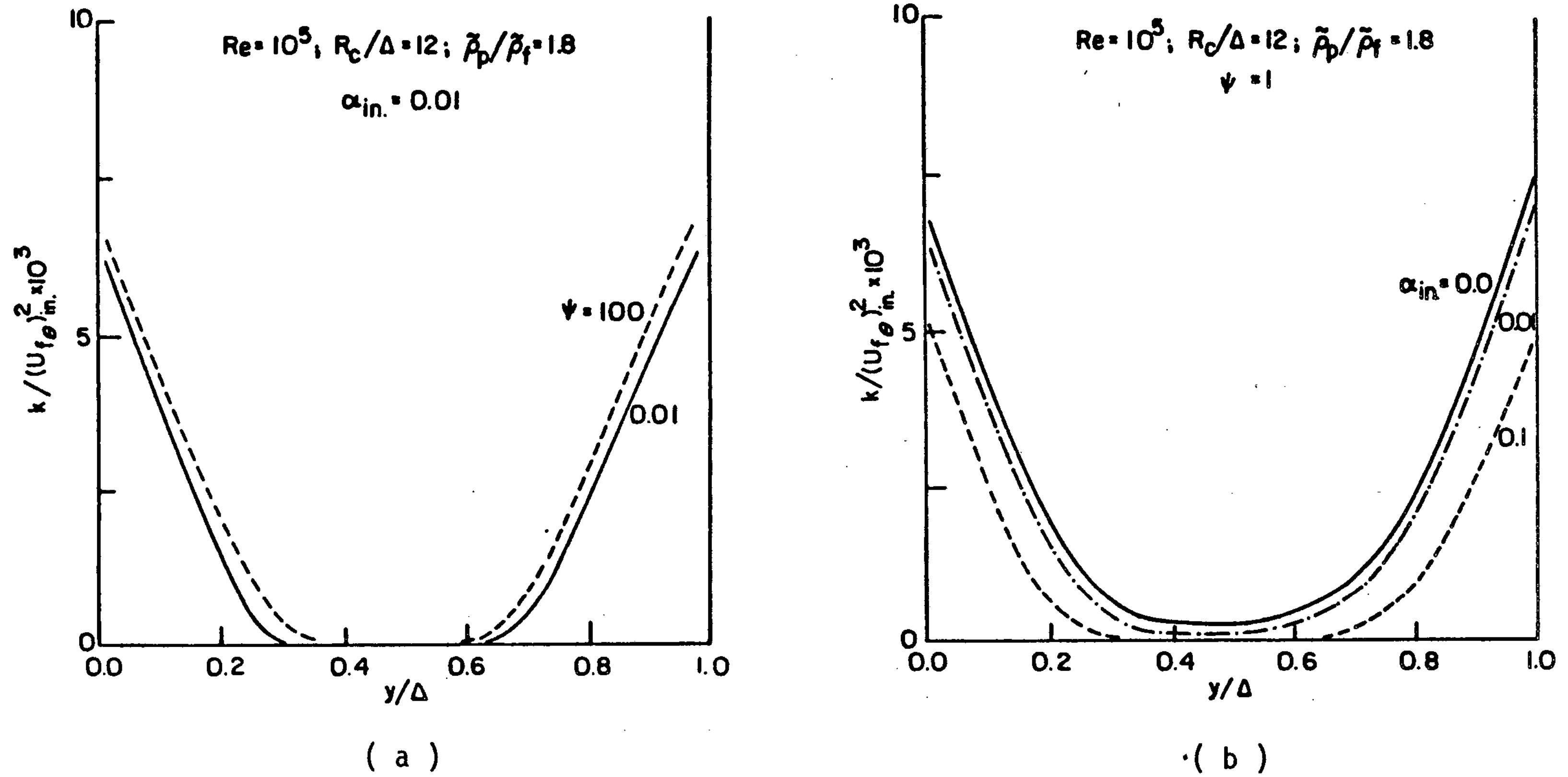

Figure 9 Transverse variation of fluid turbulent kinetic energy in the fully developed region of curved channel two-phase flow; (a) variation of ψ with α fixed; (b) variation of α with ψ fixed.

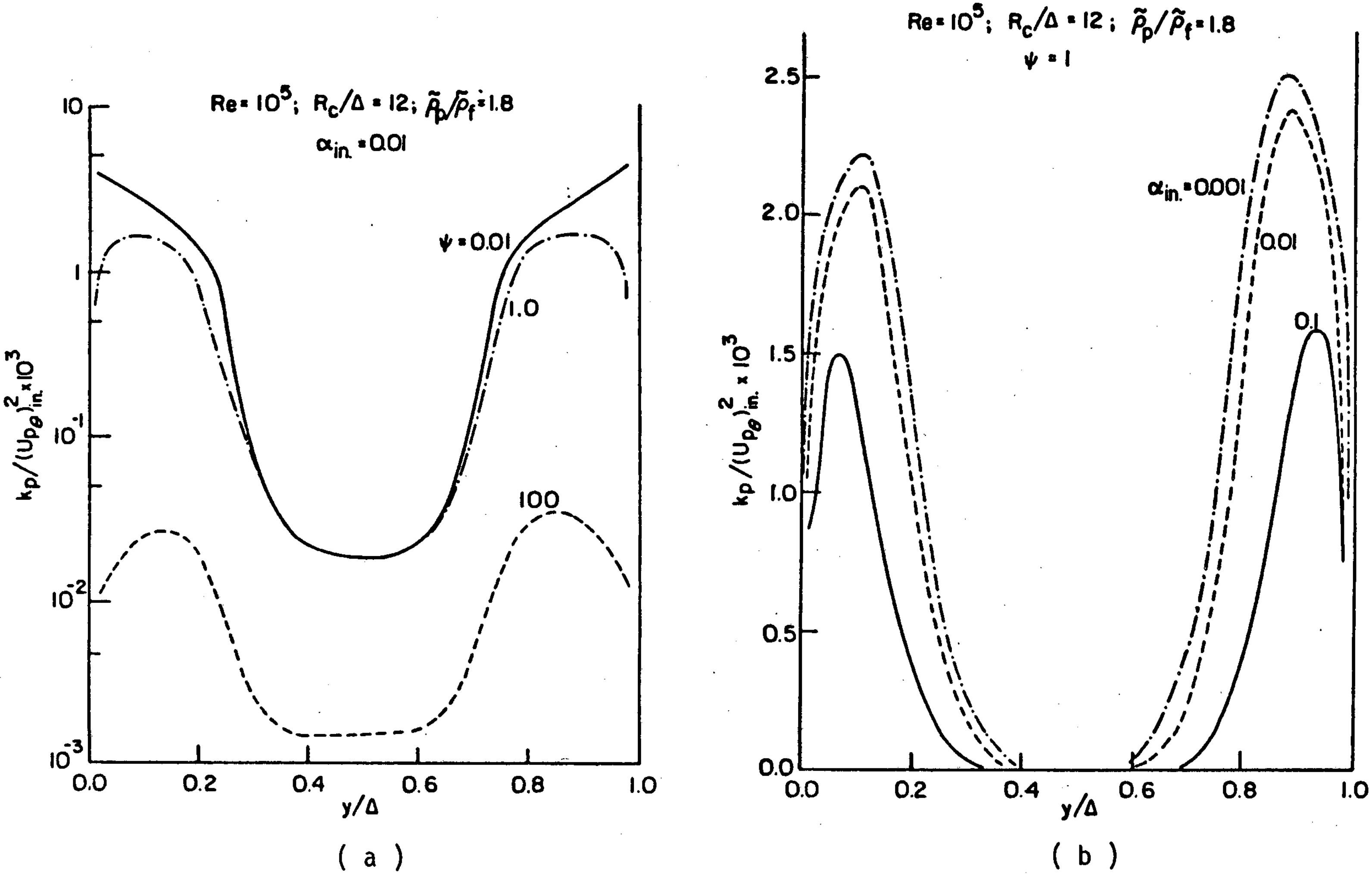

Figure 10 Transverse variation of particulate turbulent kinetic energy in the fully developed region of curved channel two-phase flow: (a) variation of ψ with α fixed; (b) variation of α with ψ fixed.

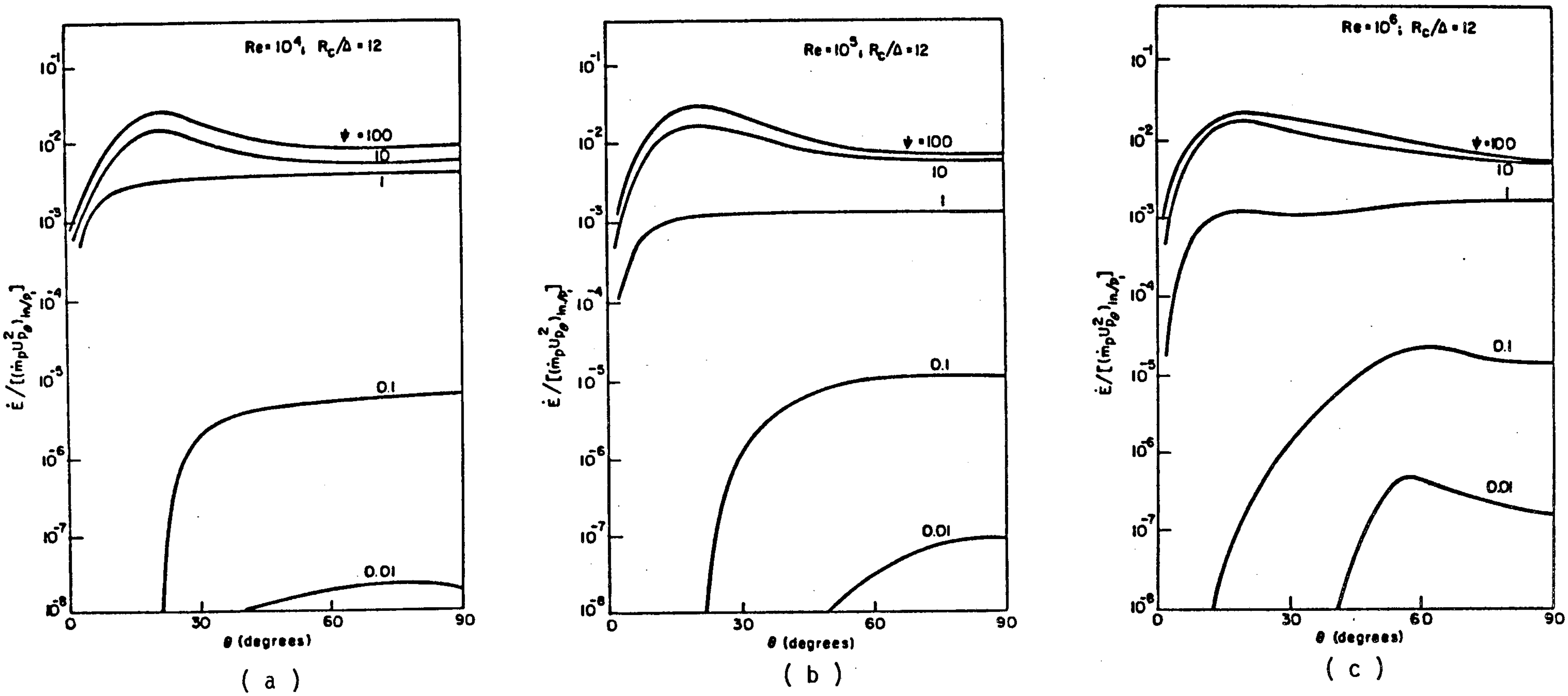

Figure 11 Longitudinal variation of normalized erosion rate at the outer wall of a curved channel two-phase flow for different particle response parameters; $\tilde{\rho}_p/\tilde{\rho}_f = 1.8$.

TECHNICAL INFORMATION DEPARTMENT
LAWRENCE BERKELEY LABORATORY
UNIVERSITY OF CALIFORNIA
BERKELEY, CALIFORNIA 94720